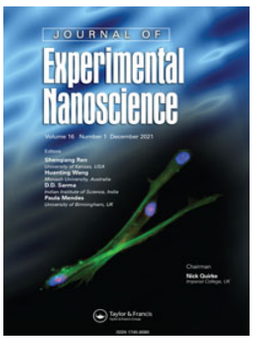

Journal of Experimental Nanoscience

ISSN: (Print) (Online) Journal homepage: https://www.tandfonline.com/loi/tjen20

Directed assembly of barium titanate nanopeapods *via* solvothermal processing with a mixed surfactant system

Alexis Blanco, Jennifer A. Webb, Rebecca R. DiMarco & John B. Wiley

To cite this article: Alexis Blanco, Jennifer A. Webb, Rebecca R. DiMarco & John B. Wiley (2021) Directed assembly of barium titanate nanopeapods *via* solvothermal processing with a mixed surfactant system, Journal of Experimental Nanoscience, 16:1, 265-277, DOI: 10.1080/17458080.2021.1962006

To link to this article: https://doi.org/10.1080/17458080.2021.1962006

JOURNAL OF EXPERIMENTAL NANOSCIENCE
2021, VOL. 16, NO. 1, 265–277
https://doi.org/10.1080/17458080.2021.1962006

Taylor & Francis
Taylor & Francis Group

Directed assembly of barium titanate nanopeapods *via* solvothermal processing with a mixed surfactant system

Alexis Blanco, Jennifer A. Webb, Rebecca R. DiMarco and John B. Wiley

Department of Chemistry and Advanced Materials Research Institute, University of New Orleans, New Orleans, LA, USA

ABSTRACT

Barium titanate ($BaTiO_3$) peapod nanocomposites were prepared by the controlled capture of nanoparticles (NPs) in scrolling hexaniobate (HNB) nanosheets. $BaTiO_3$ NPs and proton-exchanged potassium hexaniobate were treated solvothermally at 220 °C for 6 h in toluene to produce linear NP chains confined within multiwalled HNB nanoscrolls. This method consistently produced nanopeapods with average filling fractions greater than 70%. The controlled introduction of nanocomponents along with a combination of oleylamine and oleic acid surfactants was critical to the success of these reactions. The ability to form $BaTiO_3$@HNB significantly expands the number of important peapod composites accessible by the controlled NP capture.

ARTICLE HISTORY
Received 11 February 2021
Accepted 18 July 2021

KEYWORDS
Hexaniobate nanocomposites; barium titanate; nanoscrolls; synthesis; assembly

1. Introduction

Two-dimensional nanostructures have been sought for a variety of reasons including the formation of nanocomposites with 0D nanoparticle materials to develop novel structures with unique properties [1–2] and surface functionalisation [3–4]. It is known that certain nanosheets have the ability to form scrolls and that these 1D nanoscroll (NSc) structures have a range of applications in advanced materials and assembly [5–9]. Some examples of compounds that can scroll include TiO_2 [10], graphene [11], WS_2 [12], V_2O_5 [13], $K_4Nb_6O_{17}$ [1] and Ruddlesden-Popper [14] and Dion-Jacobson [15] perovskites. These types of nanomaterials have been studied due to their enhanced mechanical strength, atypical trapping behaviours as well as their applications in areas such as ion exchange, intercalation, organic–inorganic composite materials and heterogeneous catalysis [16–18]. Scrolling can also allow the production of nanocomposites *via* the controlled capture of specific guest compounds, which can lead to new materials with the improved properties [19].

$K_4Nb_6O_{17}$ is a layered compound that is biocompatible, chemically stable and displays characteristics of a wide-band semiconductor [20]. Hexaniobate nanosheets have also

CONTACT John B. Wiley jwiley@uno.edu Department of Chemistry and Advanced Materials Research Institute, University of New Orleans, New Orleans, 70148, LA, USA.

Supplemental data for this article is available online at https://doi.org/10.1080/17458080.2021.1962006.

shown evidence of photocatalytic activity under UV light [21,22]. The encapsulation or *in situ* growth of nanoparticles within the hollow spaces of the scrolls is important when considering the potential development of new nanodevices. The term 'nanopeapod' (NPP) refers to a two-part nanocomposite system of nanoparticles (pea) and nanoscrolls (pod). When nanoparticles are captured or grown within the hollow portion of the scroll, they create these nanocomposites. The confinement of different nanoparticles having varied properties, different from that of $K_4Nb_6O_{17}$, can lead to the development of novel materials that exhibit additive or completely new properties.

NPPs have several defining characteristics that can be modified such as those pertaining to NP shape, size, and type, surfactants, scroll interlayer distances, structural uniformity, and filling fraction of the NPs. Fabrication of new NPPs holds both fundamental and practical importances in various applications. Synthetic routes in the formation of NPPs have already been reported by different groups [2,19,23–30], though some of these methods may contain limitations such as application to only select combinations of nanocomponents, long-processing times, high costs, negative environmental impact and poor scalability for bulk synthesis. The combinations of exfoliation and scrolling of $K_4Nb_6O_{17}$ using tetrabutylammonium hydroxide (TBAOH) and concurrent capture or subsequent growth of various NPs offer a controlled method for the synthesis of these NPPs [2,27]. Critical to this process is the role of the surfactant; both NPs and NScs have surface groups, which are critical in the assembly processes. The absence of proper surfactants leads to clumping of NPs and the formation of empty scrolls.

The type of nanoparticle that is contained with a NPP has significant role in the defining its characteristics. Barium titanate ($BaTiO_3$) is a perovskite that is well known for its ferroelectric properties and incorporation in many devices [31]. Some $BaTiO_3$ applications include multilayer ceramic capacitors (MLCCs) [32], electro-optical devices [33], piezoelectric actuators [34] and gas sensors [35]. $BaTiO_3$ NPs have been synthesised by a variety of methods including co-precipitation [36], sol-gel [37], hydrothermal [38] and solvothermal methods [39]. NPs with sizes $\leq$ 15 nm have the potential to be encapsulated within HNB NScs. Our group has already synthesised multiple NPP structures such as gold [2], iron (II/III) oxide [25,27], cerium (IV) oxide [28] and silver NPPs [40]. Herein, we report the encapsulation of perovskite NPs where using a modified multisurfactant solvothermal method, cube-shaped $BaTiO_3$ NPs are readily captured within HNB nanoscrolls.

2. Experimental

2.1. Synthetic reagents

Potassium carbonate (K_2CO_3, 99%) and niobium oxide (Nb_2O_5, 99%) were acquired from Alfa Aesar (USA). Oleylamine (OAm, technical grade, 70%), oleic acid (OAc, 99.8%), sodium hydroxide pellets (NaOH, ACS grade), barium nitrate ($Ba(NO_3)_2$, 99%), butanol (ACS reagent, 99%), decanol (99%), titanium (IV) butoxide (reagent grade, 99%), toluene (certified ACS, 99.8% anhydrous), acetone (certified ACS, 99%), and TBAOH30-hydrate were purchased from Sigma-Aldrich (USA). Deionised water was obtained *via* reverse osmosis.

2.2. Barium titanate nanoparticles

$BaTiO_3$ NPs with sizes ranging from 10 to 13 nm were synthesised *via* known solvothermal methods [41] in a stainless steel autoclave (Parr model 4749 A) with a Teflon liner.

NaOH (12.5 mmol) was added to distilled water (2 mL) in vial (I) and $Ba(NO_3)_2$ (1 mmol) was added to distilled water (3 mL) in vial (II). A mixture of oleic acid (2.5 mL) and butanol (2 mL) was prepared separately in vial (III), and decanol (3 mL) was added to titanium (IV) butoxide (1 mmol) in vial (IV). The vials were combined in the reverse order in which they were made, i.e. (III) to (IV), (II) to (IV) and (I) to (IV). The resulting white mixture was stirred vigorously for 5 min *via* magnetic stirring. This was then transferred to the Teflon liner and placed into the autoclave. The autoclave was sealed, and the mixture was heated to 180 °C for 18 h. $BaTiO_3$ NPs were collected, washed three times with toluene *via* centrifugation (6000 RPM) for 10 min, and dispersed in a non-polar solvent (toluene). **Caution:** *Soluble barium salts are highly toxic and should be handled with extreme caution.*

2.3. $K_4Nb_6O_{17}$

Crystalline samples of layered $K_4Nb_6O_{17}$ were prepared by a high-temperature ceramic method [1]. K_2CO_3 and Nb_2O_5 (molar ratio 1.4:1) were placed in a ball mill within a stainless steel planetary cell (50 mL). Zirconia ball media (10 balls, 5 mm) were added to the cell and placed in a ball mill (Spex Industrial Inc., Spex Mixer 8000) for 15 min. After the allotted time, the mixture was then placed in an alumina crucible. An initial excess of 10% K_2CO_3 was included to compensate for the volatilisation during high-temperature synthesis. This mixture was heated at 900^{o}C for 1 h and cooled to room temperature. A further 10% of K_2CO_3 was then added to prevent the formation of potassium-deficient phases. The mixture was milled again for 15 min. The sample was placed in an alumina crucible where it was heated for 2 days at 1050^{o}C, followed by 1 h at 1100^{o}C. The sample was cooled to room temperature, washed *via* vacuum filtration with deionised water (twice) and water/acetone (once), and then dried overnight at 75^{o}C.

2.4. Acid exchange of $K_4Nb_6O_{17}$

To obtain the proton-exchange form of HNB, $H_xK_{4-x}Nb_6O_{17}$, 1 g of $K_4Nb_6O_{17}$ powder was combined with 8 mL of a 6 M HCl in a stainless steel autoclave (Parr model 4749 A) with a PTFE liner and heated at 90^{o}C for 2 days. The product was then washed *via* centrifugation (6000 RPM) for 10 min with deionised water (twice) and water/acetone (once) and dried overnight at 75^{o}C.

2.5. Solvothermal preparation of $BaTiO_3$@HNB nanopeapods

0.1 g $H_xK_{4-x}Nb_6O_{17}$, 0.2 g TBAOH, 5 mL OAm, 2 mL OAc and 3 mL of toluene were added to a PTFE Teflon liner and stirred for 1 h at room temperature. After the mixture was stirred, 50 mg of $BaTiO_3$ NPs was dispersed in 2 mL of toluene *via* sonication (2 min) in a separate vial and added to the $H_xK_{4-x}Nb_6O_{17}$ mixture with no additional stirring. The liner was then transferred to a stainless steel autoclave (Parr), sealed and heated to 220^{o}C for 6 h. The resulting product was washed with toluene (3×) and separated *via* centrifugation (13,000 RPM). It was found that the solid precipitate collected at the bottom of the centrifugation tube consisted mainly of NPPs. For this reason, studies were done mostly on samples collected from the lower region of the tube. Other reactions were also investigated leading to the optimal synthesis conditions. These other reactions are presented below.

2.6. Characterisation

The morphologies of the products were characterised with a JEOL 2010 (USA) transmission electron microscope (TEM) operated at an accelerating voltage of 200 kV; the TEM was equipped with a Gatan slow-scan CCD camera and an EDAX Genesis (USA) energy-dispersive spectroscopy (EDS) system. TEM images of NPPs were analysed with the ImageJ software to find interlayer spacing values of the multiwalled $BaTiO_3$@HNB NPPs, determine inner and outer NPP diameters, calculate filling fractions for the NPPs and determine $BaTiO_3$ NP sizes. X-ray powder diffraction (XRD) data were collected for the host, protonated hexaniobate and $BaTiO_3$ NNPs on a Philips X'Pert diffractometer utilising Cu Kα radiation ($\lambda = 1.5418$ Å) and a curved graphite monochromator at a voltage of 45 kV and a current of 40 mA.

3. Results

3.1. Barium titanate nanoparticles

$BaTiO_3$ NPs, synthesised *via* a modified literature procedure [41], exhibited a cubic shape with an average size of 13 ± 2 nm; TEM images of the $BaTiO_3$ NPs are shown in Figure 1A along with a size distribution diagram (Figure 1(B)). The observed XRD patterns for the $BaTiO_3$ particles can be seen in Figure S1A (figure found on-line in supplemental data) and are in good agreement with the reference pattern for bulk $BaTiO_3$ in Figure S1B; line broadening is consistent with the smaller sized $BaTiO_3$ nanoparticles (Figure S1A).

Varied synthetic routes were investigated to determine the optimal NP composition for the capture within the hexaniobate nanosheet system. Synthesis of $BaTiO_3$ NPs required the use of oleic acid as the surfactant, whereas the formation of nanoscrolls typically uses oleylamine. Oleylamine, however, readily reacts with the oleic acid located on the surface of the $BaTiO_3$ particles resulting in extensive NP agglomeration. Adjusted surfactant ratios, therefore, were examined in the search for optimal NPs. Table 1 highlights the varied synthetic routes used in these early studies, and Figure S2 shows some of the resulting NPs.

Nanoscrolls are typically between 0.1 and 1 μm in length with 2 to 6 inner spiral layers, wall thicknesses of 10–20 nm and inner diameters ranging from 10 to 25 nm. Therefore, the size of the $BaTiO_3$ NPs that were required for encapsulation had to range from 7 to 15 nm. Varying the surfactant concentration produced unsuitable $BaTiO_3$ NPs that had either extremely large or small sizes (Figure S2). Particles that were synthesised without the use of oleic acid (Sample 1, Supplemental data) were large (> 20 nm, Figure S2A) and had spherical morphologies, whereas particles that were synthesised using a 50:50 mixture of both surfactants (Sample 2, Supplemental data) (Figure S2B), had a range of sizes from 8 to 50 nm with various morphologies. The best NPs for this study were formed utilising only oleic acid as the surfactant (Figure 1).

Table 1. The different ratios of oleylamine versus oleic acid that were used when designing a compatible barium titanate particle for hexaniobate nanoscrolls.

Sample	Oleic acid ratio (%)	Oleylamine ratio (%)
1	0	100
2	50	50
3	100	0
4	100	0
5	60	40

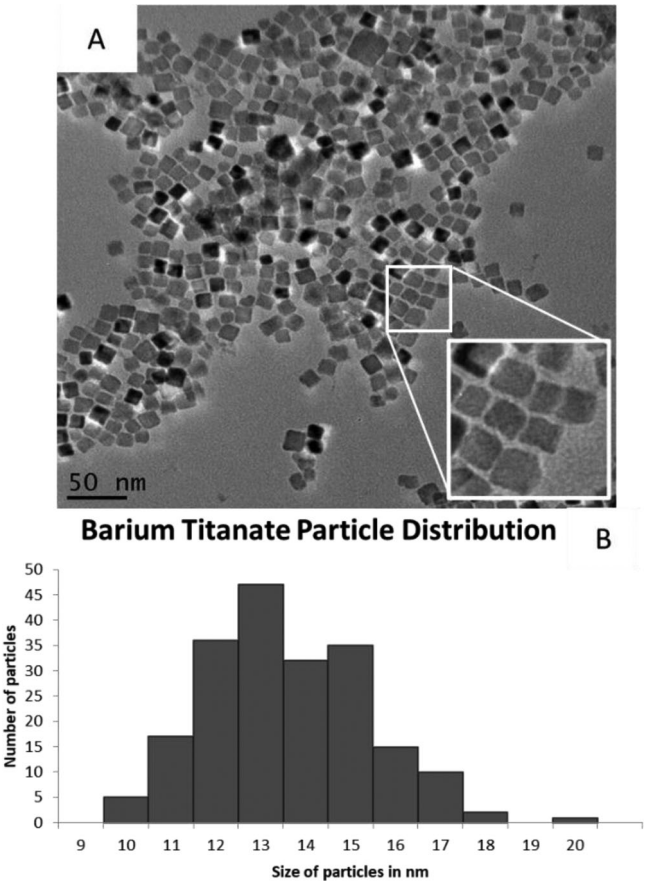

Figure 1. Barium titanate nanocubes. (A) Monodispersed cubic particles can be seen in the TEM images. (B) Size distribution of 200 measured particles with an average width of 13 ± 2 nm.

3.2. $BaTiO_3$ hexaniobate nanopeapods

Earlier methods of NPP fabrication [2] worked well with NPs that contained the same surfactant as the NScs. This can be seen with studies from our group where oleylamine was the surfactant when making the NP of choice [2,27,28]. Since the formation of monodispersed oleylamine-capped $BaTiO_3$ NPs did not readily occur, a different approach to the synthesis of $BaTiO_3$ HNB NPPs was carried out where modification of the NPP system was studied as opposed to the modification of the NP. Oleic acid and oleylamine were used in various ratios to determine the best parameters for encapsulation (Table 2). Also, other NPP synthesis variations were explored including reaction time, surfactant amounts, solvent system and mixing times (Table 2). The initial reaction conditions (reactions 1–9) were unsuccessful in encapsulation (Figure S3 and Table 2); extensive agglomeration and loose-forming scrolls could be seen throughout all early attempts at encapsulation.

The production of NPPs is not only influenced by the amount of surfactant, NP size, solvent, reaction time and temperature, but also other factors such as the presence of TBAOH and types of surfactants play crucial roles as well. Within this study, TBAOH, the exfoliating agent, separates the hexaniobate sheets from each other, while oleylamine and oleic acid play dual roles as intercalant and surfactant. To better understand these limitations, experiments were performed in a water-based system without the use of the

Table 2. All the major synthetic routes that were taken when optimising the formation of $BaTiO_3$@hexaniobate nanopeapods. The final reaction, Reaction 14, was the best, producing the most encapsulation.

Reaction	Oleic acid ratio (mL)	Oleylamine ratio (mL)	Solvent	Stir (mins)	Particles present during stir	Oven time (hrs)	Oven temp. (°C)
1	0	5	Toluene	60	Yes	6	220
2	2	3	Toluene	60	Yes	10	220
3	2	3	Toluene	60	Yes	8	220
4	1	4	Toluene	60	Yes	6	220
5	4	1	Toluene	60	Yes	6	220
6	0.5	5	Toluene	60	Yes	6	220
7	5	2	Toluene	60	Yes	6	220
8	2	3	Hex/EtOH	60	Yes	6	220
9	2	3	Hexane	60	Yes	6	220
10	2	5	Toluene	5	Yes	6	220
11	1	5	Toluene	60	Yes	6	220
12		Water		4320	Yes	0	N/A
13	2	5	Toluene	60	Yes	6	220
14	2	5	Toluene	60	No	6	220

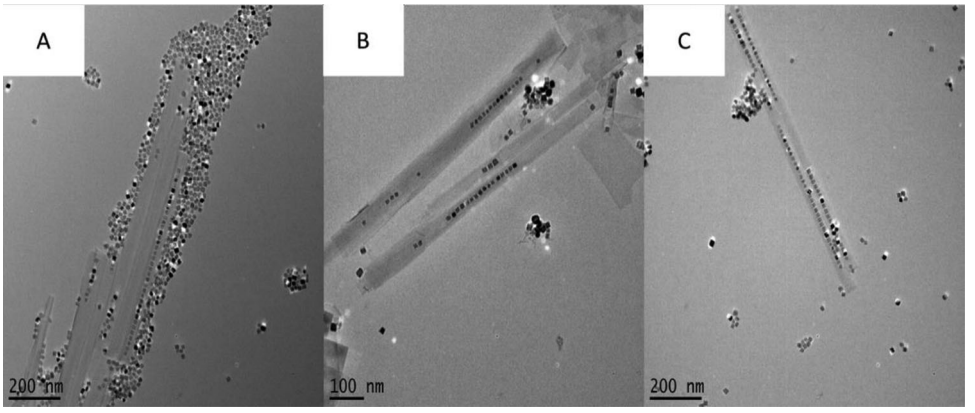

Figure 2. Figure showing the effects of stirring before heating when synthesising $BaTiO_3$@hexaniobate nanopeapods. (A) Reaction 10, sample was only stirred for 5 min with barium titanate particles introduced. (B) Reaction 13, sample was stirred for 1 h with particles introduced. (C) Sample with stirred for 1 h without the particles added. After the 1-h time passed, sonicated particles were added in before heating occurred.

surfactant. Formation of nanoscrolls was seen using this non-surfactant method but the resulting scrolls were not tightly wound (Figure S4) and subsequent reactions to form NPPs were not successful.

Further studies examined the role of reaction conditions for the optimal synthesis of NPPs. Here, it was shown that strict control of nanoparticle introduction was significant in the production of NPPs. Figure 2 shows the TEM images of $BaTiO_3$@hexaniobate NNP samples that were synthesised using various stir times. Samples that underwent the typical NPP synthetic route [27] (Figure 2(B)), including 1-h stirring of the mixture along with particles prior to the solvothermal treatment, showed agglomeration of NPs and low levels of nanoparticle encapsulation. When the system was stirred for only 5 min (Figure 2(A)) with particles present, evidence of the agglomeration was still present but with the improved encapsulation. The addition of particles immediately after the 1-h stir showed the best NP encapsulation (Figure 2(C)) and a decrease in agglomeration. Furthermore, the optimal synthetic route used a surfactant ratio of 1:0.4 (5 mL:2 mL) of oleylamine to oleic acid with particles being added after the 1-h stirring stage, immediately before the solvothermal processing. Figure 3 presents a typical high-yield $BaTiO_3$@hexaniobate NPP

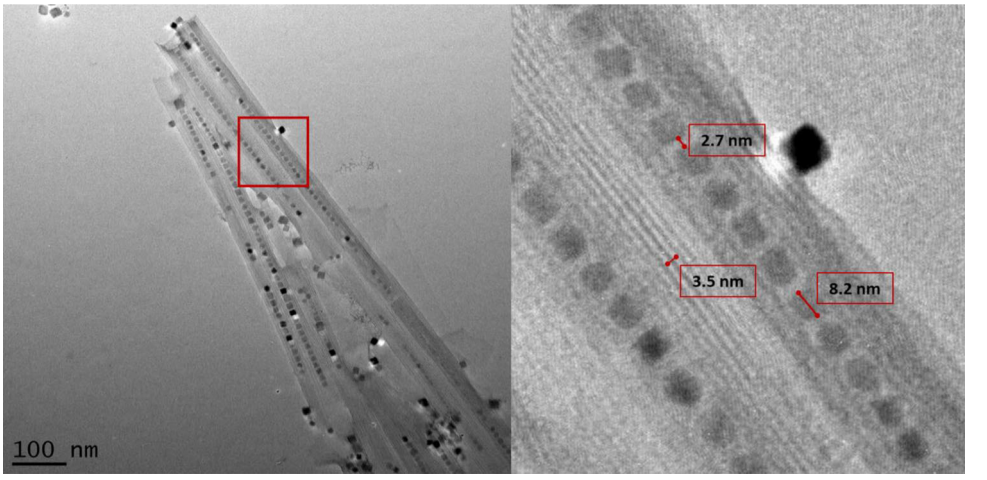

Figure 3. $BaTiO_3$ nanopeapods made using the optimal synthetic pathway (Table 2, Reaction 14). Left. Image of four adjacent nanopeapods. Right. Higher magnification image shows scroll layer spacing, interparticle distance and a typical size of nanoparticles located within the hexaniobate nanoscroll.

sample. Close examination of the peapods showed that typical captured $BaTiO_3$ NP sizes were 8–9 nm in size, interparticle distances averaged about 2.7 nm and the layer spacing in nanopeapod scrolls was ~3.5 nm.

$BaTiO_3$@hexaniobate NPPs contained a certain number of NPs based on the length of the nanoscroll, 10 NPs for the smaller scrolls (~150 nm in length) to 70 NPs for larger scrolls (over 1 µm in length) with an interparticle space of about 2–3 nm. Additional NPPs can be seen in Figure 4 showing variations of the sizes on NPPs obtained and the number of encapsulated particles. Figure 4B highlights a $BaTiO_3$@hexaniobate NPPs showing a NPP over 1 µm in length. If smaller NPs are encapsulated, there is a chance that the particles can align themselves in two separate rows; this can be seen in Figure 4C (inset) where a set of 8-nm particles occur in two separate rows.

Overall, statistical evaluation of the encapsulated nanoparticles and the spacing between them can be seen in Figure 5. Using these statistical values, it was possible to obtain filling fractions for the NPPs. The filling fraction was determined for 150 NPPs. The pie chart in Figure 6 shows the filling fraction distribution seen in the NPPs. The majority of the NPPs have filling fractions over 70%.

The XRD pattern for the NPPs is shown in Figure 7A with corresponding patterns for both $BaTiO_3$ NPs and HNB nanoscrolls, Figure 7B,C, respectively. Comparing Figure 7A,B, evidence for the $BaTiO_3$ NPs can be seen in the NPP sample, though the potassium hexaniobate is more dominant in the pattern. The peaks located in the lower angle reflection of Figure 7A,C are the 'fingerprint' regions of the scrolls. Each one of the peaks in this area is indicative of the intercalated scrolls. These data are consistent with the formation of the $BaTiO_3$@hexaniobate NPPs.

4. Discussion

Both TBAOH and the surfactants (oleylamine and oleic acid) are essential to the formation of the $BaTiO_3$@hexaniobate NPPs. TBAOH promotes the necessary exfoliation and scrolling needed from the thicker hexaniobate crystallites, whereas the surfactant aids in the functionalisation of both the nanoparticles and nanoscrolls. $BaTiO_3$ NPs are

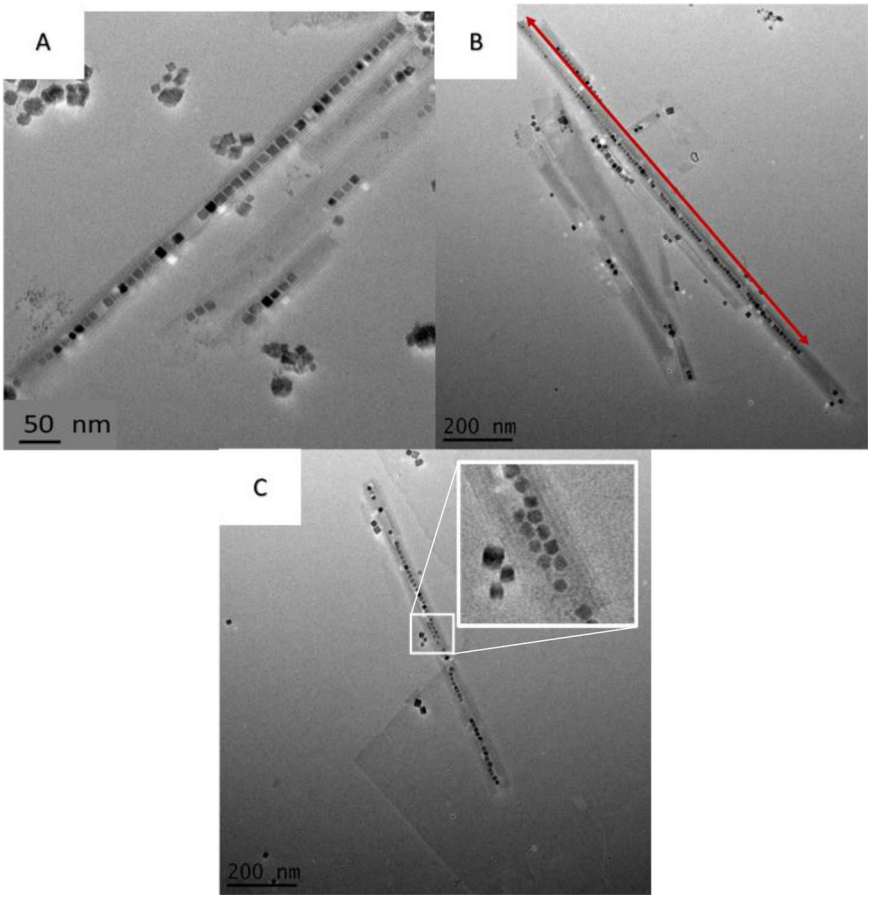

Figure 4. Additional $BaTiO_3$@hexaniobate samples. (A) The capture of larger $BaTiO_3$ particles. (B) An exceptionally long (> 1 μm) NPP is observed. (C) Two rows of encapsulated $BaTiO_3$ nanoparticles can be seen in the centre of the nanoscroll.

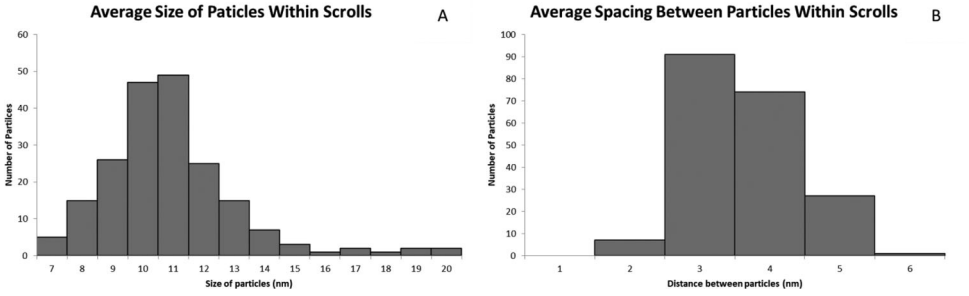

Figure 5. Overall statistics obtained from NPPs produced after successful replication of synthesis (Reaction 14 from Table 2). Average particle size located within the scrolls was 10 ± 2 nm with an average of 27 ± 14 particles encapsulated. These particles also had an average spacing of 2.7 ± 0.7 nm.

made in a system where oleic acid is used predominantly as the surfactant. Attempts were made to replicate these particles by substituting oleic acid with oleylamine, however this yielded NPs whose sizes were greater than 20 nm (Figure S2A). The difference between oleic acid and oleylamine is the functional group located at the head of the aliphatic chain; oleic acid has a carboxylic acid group, whereas oleylamine has an

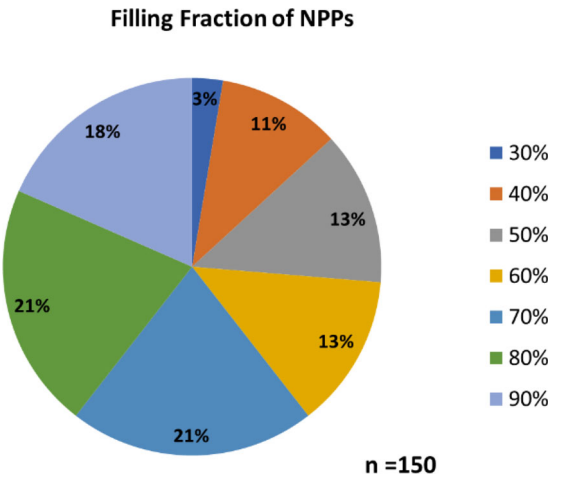

Figure 6. Filling fractions of the $BaTiO_3$@HNB NPPs with 150 NPPs considered. Calculations based on the volume occupied by particles inside scrolls.

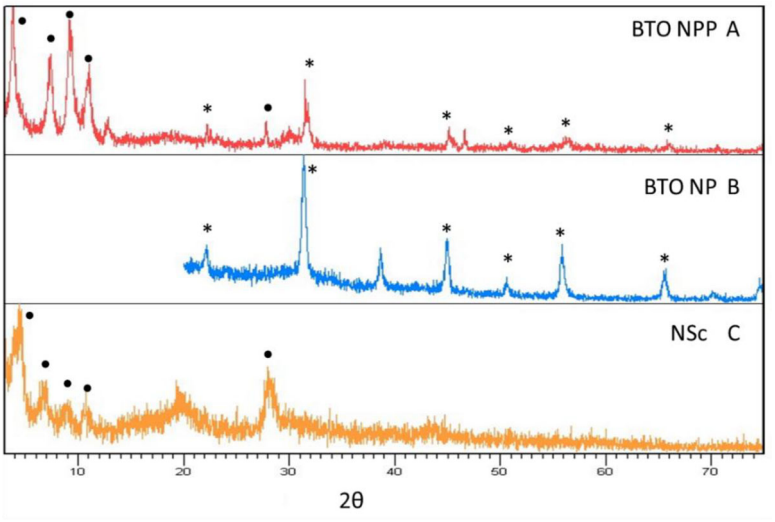

Figure 7. Observed XRD patterns of the (A) synthesised $BaTiO_3$@hexaniobate nanopeapods, (B) barium titanate nanoparticles (*) that were used in the synthesis and (C) observed pattern of potassium hexaniobate scrolls (●) alone. A slight zero-shift in the data is attributed to sample displacement.

amine group. The negative charge associated with the amine functional group of oleylamine potentially had adverse effect on the particles that lead to the large growth. More systems were then tested where both oleic acid and oleylamine were used as the surfactant in the $BaTiO_3$ NP synthesis (Table 1). The sizes of these NPs were very broad, ranging from ~8 to 20 nm (Figure S2). None of these systems lead to successful encapsulation.

An understanding of the hexaniobate scrolling process is important when attempting to modify nanopeapod production. Investigations on bulk hexaniobate nanoscroll and CeO_2 NPP systems [28] revealed that instead of the nanoscrolls and NPPs being produced from individual exfoliated nanosheets, they develop from larger hexaniobate crystallites, which are broken off during synthesis. In the case of the NPPs, the NPs preassembly

along a crystal edge prior to peapod formation and detachment [28]. Further, results from our group's time-dependent studies show evidence of the partial formation of nanoscrolls on the surface of the hexaniobate nanosheet with typical sizes of the crystallites being as much as 50 µm on an edge, but resulting in nanoscrolls that are much smaller in length [27]. Other factors that influence the size of the nanoscrolls include temperature, pressure, the rate of scrolling, the type of surfactant used to aid in intercalation and the presence of any structural defects on the nanosheets themselves.

Previous successful NPPs syntheses, especially *in situ* methods, contain a stirring step within the synthesis before the actual heating phase [2]. Stirring aids in the initial reaction of the nanosheets with the exfoliants and surfactant. Hexaniobate nanosheets are attached to a layered crystallite system before exfoliation. In the hexaniobate-layered system, only the edges, top and bottom layers are considered to be reactive. This exfoliation is concurrent to scrolling, which is aided by the long-chain surfactant used in the synthesis. However, when synthesising NPPs, the nature of the NP must also be taken into consideration. The surfactant used in producing $BaTiO_3$ NPs in this synthesis is oleic acid. Hexaniobate nanoscrolls are made in a system that uses oleylamine as the surfactant. Oleic acid, as the name suggests, is an acid, while oleylamine is a base. The synthesis of hexaniobate nanoscrolls also uses TBAOH, which is used as the exfoliant and is also a base. Hexaniobate nanoscrolls are made in a basic system as opposed to $BaTiO_3$, which is acidic. During the initial formation of nanopeapods (1-h stirring phase before heating) TBA^+ ions react with the negatively charged edges of the nanosheets. It is expected that this reaction separates a sheet from either the top or bottom of the crystallite and starts the initial scrolling step. Oleylamine is then introduced in the now revealed layer to further the scrolling and expand the interlayer spacing within the nanoscroll. This overall system is basic in nature due to both TBAOH and oleylamine being present at the same time. If NPs are being introduced, whose nature is acidic, this can cause a change in the initial reaction, negatively impacting the formation of the NPPs.

$BaTiO_3$ NPs are coated with a layer of oleic acid. The introduction of these NPs to a basic environment without strict control of processing steps can lead to agglomeration of the particles due to loss of surface groups. This was seen when attempting to make $BaTiO_3$@hexaniobate NPPs by introducing $BaTiO_3$ NPs in the stirring phase of the synthesis (Figure 2(A,B)). Figure 2A shows a modified stirring time of 5 min before the solvothermal treatment. An increase in the number of the NPPs was seen; however, particle agglomeration was still present. The agglomeration is a result of the basic system present, while particles were introduced. To potentially counter the agglomeration, particles were introduced after the 1-h stirring phase. This led to a significant increase in encapsulation of $BaTiO_3$ NPs with decreased agglomeration seen throughout the sample (Figures 2(C) and 3).

To understand the mechanism behind the formation of the NPPs using this method, it is important to consider how oleic acid and oleylamine function in the presence of one another. The reaction of both oleylamine and oleic acid in a 1:1 molar ratio has already been documented [42,43]. When oleic acid is added to a system of oleylamine in a 1:1 ratio, the carboxylic acid group deprotonates in the presence of the amine. This then forms a carboxylic anion along with a quaternary ammonium cation. Reaction 1 shows the overall scheme of the reaction that takes place.

$$C_{17}H_{33}COOH + C_{18}H_{35}NH_2 \rightarrow C_{17}H_{33}COO^- + C_{18}H_{35}NH_3^+ \quad (1)$$

It is possible that when $BaTiO_3$ NPs particles are added to a NPPs synthesis without the presence of any excess oleic acid, oleylamine in the system reacts and removes the

oleic acid on the surface of the NPs, leaving exposed facets of the NPs. These exposed facets can then react with each other, which leads to growth and agglomeration of the particles. This would explain the low yield in initial attempts making $BaTiO_3$@hexaniobate NPPs. The addition of excess oleic acid to the NPPs system increased the number of NPPs obtained but agglomeration was still visible. As mentioned before, the 1-h stirring phase of the synthesis allows for exfoliation and preliminary scrolling of the nanosheets. However, when having both oleic acid and oleylamine in the system while stirring, the formation of Reaction 1 will also be present. The presence of the anion and the cation in this system decreased the number of nanoscrolls that would have been produced when compared to a typical nanoscroll reaction. Also, it is suggested that the oleic acid surrounding the NPs and the excess oleic acid added to the reaction can react with oleylamine to form both anions and cations, even after stirring, which can lead to open facets in the NPs but not as severely. This is the possible reason why increase in NPPs was observed but with small agglomeration still present throughout. The main contributing factor when taking this route was that the nanosheets had enough time to react with oleylamine to start the initial scrolling process. With the nanosheets sequestering the majority of the oleylamine, $BaTiO_3$ NPs were protected from reaction with the oleylamine, and this allowed for effective NP encapsulation.

5. Conclusions

In summary, $BaTiO_3$ NPPs have been prepared by solvothermal methods using a mixture of oleic acid and oleylamine. $BaTiO_3$ NPs with sizes measuring ~10 nm were successfully encapsulated within hexaniobate nanoscrolls. Attempts at making $BaTiO_3$ nanoparticles with the use of just the surfactant, oleylamine, were too large and not suitable for encapsulation. Similarly, the use of oleic acid, when synthesising hexaniobate nanoscrolls, led to the formation of loose, non-uniform scrolls. Oleic acid and oleylamine can react, such that oleylamine can remove oleic acid from $BaTiO_3$ nanoparticles leading to NP agglomeration. Stirring of the starting materials is essential for the initial scrolling process to take place. However, as the results showed, the addition of the particles too early within this step led to heavy agglomeration in the resulting attempt at encapsulation. This was due to the oleylamine reacting with the oleic acid on the surface of the particles. The addition of the particles after this stirring phase proved to be ideal to avoid agglomeration and to still allow the preliminary scrolling process to occur. For these reasons, the ratio system of both oleic acid and oleylamine was used in the overall nanopeapods synthesis but with strict control over the timing of NP introduction in the process.

The successful encapsulation of $BaTiO_3$ nanoparticles within hexaniobate nanoscrolls has added another valuable composite to known nanopeapod systems. The combination of $BaTiO_3$ and $K_4Nb_6O_{17}$ makes it a unique hybrid system with potential applications in nanoscale polarisable materials.

Disclosure statement

No potential conflict of interest was reported by the authors.

Funding

This material is based upon work supported by the National Science Foundation under grant CHE-2004178. JAW is grateful for the AMRI summer research internship and RRD thanks the National Science Foundation for support through the REU program, grant DMR-1262904.

References

1. Adireddy S, Yao Y, He J, et al. Rapid solvothermal fabrication of hexaniobate nanoscrolls. Mater Res Bull. 2013;48(9):3236–3241.
2. Adireddy S, Carbo CE, Rostamzadeh T, et al. Peapod-type nanocomposites through the in situ growth of gold nanoparticles within preformed hexaniobate nanoscrolls. Angew Chem Int Ed Engl. 2014;53(18):4614–4617.
3. Thurakkal S, Zhang XY. Recent advances in chemical functionalization of 2D black phosphorous nanosheets. Adv Sci. 2020;7(2).
4. Ma XY, Wu SY, Yi ZM, et al. The effect mechanism of functionalization on thermal conductivity of boron nitride nanosheets/paraffin composites. Int J Heat Mass Tran. 2019;137:790–798.
5. Jin YK, Xue QZ, Zhu L, et al. Self-assembly of hydrofluorinated janus graphene monolayer: a versatile route for designing novel janus nanoscrolls. Sci Rep. 2016;6:26914.
6. Liu HD, Le T, Zhang L, et al. Carbon nanoscrolls: synthesis and applications. J Mater Sci: Mater Electron. 2018;29(22):18891–18904.
7. Qayyum MS, Hayat H, Matharu RK, et al. Boron nitride nanoscrolls: structure, synthesis, and applications. Appl Phys Rev. 2019; 6(2).
8. Islam M, Rahman MM, Chowdhury MM, et al. Graphene nanoscrolls via electric-field-induced transformation of water-submerged graphene nanoribbons for energy storage, nanofluidic, and nanoelectronic applications. ACS Appl Nano Mater. 2019;2(9):5857–5870.
9. Chervy P, Petcut C, Rault D, et al. Organic nanoscrolls from electrostatic interactions between peptides and lipids: assembly steps and structure. Langmuir. 2019;35(32):10648–10657.
10. Sahin EA, Mert BD, Doslu ST, et al. Investigation of the hydrogen evolution on Ni deposited titanium oxide nano tubes. Int J Hydrogen Energy. 2012;37(16):11625–11631.
11. Wang L, Yang P, Liu Y, et al. Scrolling up graphene oxide nanosheets assisted by self-assembled monolayers of alkanethiols. Nanoscale. 2017;9(28):9997–10001.
12. Li YD, Li XL, He RR, et al. Artificial lamellar mesostructures to WS(2) nanotubes. J Am Chem Soc. 2002;124(7):1411–1416.
13. Lutta ST, Dong H, Zavalij PY, et al. Synthesis of vanadium oxide nanofibers and tubes using polylactide fibers as template. Mater Res Bull. 2005;40(2):383–393.
14. Schaak RE, Mallouk TE. Prying apart Ruddlesden-Popper phases: exfoliation into sheets and nanotubes for assembly of perovskite thin films. Chem Mater. 2000;12(11):3427–3434.
15. Maeda K, Mallouk TE. Comparison of two- and three-layer restacked Dion-Jacobson phase niobate nanosheets as catalysts for photochemical hydrogen evolution. J Mater Chem. 2009;19(27): 4813–4818.
16. An YL, Wang DJ, Wu C. Ion-exchange between $Na_2Ti_3O_7$ and $H_2Ti_3O_7$ nanosheets at different pH levels: an experimental and first-principles study. Physica E. 2014;60:210–213.
17. Kwak IH, Abbas HG, Kwon IS, et al. Intercalation of cobaltocene into WS_2 nanosheets for enhanced catalytic hydrogen evolution reaction. J Mater Chem A. 2019;7(14):8101–8106.
18. Bizeto MA, Alves WA, Barbosa CAS, et al. Evaluation of hexaniobate nanoscrolls as support for immobilization of a copper complex catalyst. Inorg Chem. 2006;45(16):6214–6221.
19. Yao Y, Chaubey GS, Wiley JB. Fabrication of nanopeapods: scrolling of niobate nanosheets for magnetic nanoparticle chain encapsulation. J Am Chem Soc. 2012;134(5):2450–2452.
20. Jung YH, Shim HK, Kim HW, et al. Photochemical hydrogen evolution in $K_4Nb_6O_{17}$ semiconductor particles sensitized by phosphonated trisbipyridine ruthenium complexes. B Korean Chem Soc. 2007;28(6):921–928.
21. Nunes BN, Patrocinio AOT, Bahnemann DW. Influence of the preparation conditions on the morphology and photocatalytic performance Pt-modified hexaniobate composites. J Phys-Condens Matter. 2019;31(39).
22. Nunes BN, Haisch C, Emeline AV, et al. Photocatalytic properties of layer-by-layer thin films of hexaniobate nanoscrolls. Catal Today. 2019;326:60–67.
23. Xiao ZH, Ning GQ, Yu ZQ, et al. MnO@graphene nanopeapods derived via a one-pot hydrothermal process for a high performance anode in Li-ion batteries. Nanoscale. 2019;11(17):8270–8280.
24. Shinohara H. Peapods: exploring the inner space of carbon nanotubes. Jpn J Appl Phys. 2018;57(2): 020101.
25. Rostamzadeh T, Khan MSI, Riche K, et al. Rapid and controlled in situ growth of noble metal nanostructures within halloysite clay nanotubes. Langmuir. 2017;33(45):13051–13059.
26. Byoun W, Yoo H. Peapod assemblies of Au and Au/Pt nanoparticles encapsulated within hollow silica nanotubes. Chemistryselect. 2017;2(8):2414–2419.

27. Adireddy S, Carbo CE, Yao Y, et al. High-Yield solvothermal synthesis of magnetic peapod nanocomposites via the capture of preformed nanoparticles in scrolled nanosheets. Chem Mater. 2013; 25(19):3902–3909.
28. Rostamzadeh T, Adireddy S, Chin CDW, et al. Formation of mixed-metal ceria nanopeapod composites within scrolled hexaniobate nanosheets. Chemnanomat. 2019;5(11):1373–1380.
29. Chin CDW, Akbarian-Tefaghi S, Reconco-Ramirez J, et al. Rapid microwave synthesis and optical activity of highly crystalline platinum nanocubes (vol 8, pg 71, 2018). MRS Commun. 2018;8(4): 1483–1483.
30. Hamdi J, Blanco AA, Diehl B, et al. Room-temperature aqueous Suzuki-Miyaura cross-coupling reactions catalyzed via a recyclable palladium@halloysite nanocomposite. Org Lett. 2019;21(10): 3471–3475.
31. Hwu JM, Yu WH, Yang WC, et al. Characterization of dielectric barium titanate powders prepared by homogeneous precipitation chemical reaction for embedded capacitor applications. Mater Res Bull. 2005;40(10):1662–1679.
32. Schneller T, Halder S, Waser R, et al. Nanocomposite thin films for miniaturized multi-layer ceramic capacitors prepared from barium titanate nanoparticle based hybrid solutions. J Mater Chem. 2011;21(22):7953–7965.
33. Mimura K, Hiramatsu K, Moriya M, et al. Optical properties of transparent barium titanate nanoparticle/polymer hybrid synthesized from metal alkoxides. J Nanopart Res. 2010;12(5):1933–1943.
34. Yang D, Ge FX, Tian M, et al. Dielectric elastomer actuator with excellent electromechanical performance using slide-ring materials/barium titanate composites. J Mater Chem A. 2015;3(18): 9468–9479.
35. Wang J, Wan H, Lin QH. Properties of a nanocrystalline barium titanate on silicon humidity sensor. Meas Sci Technol. 2003;14(2):172–175.
36. Fomekong RL, You SJ, Enrichi F, et al. Impact of oxalate ligand in Co-precipitation route on morphological properties and phase constitution of undoped and Rh-doped $BaTiO_3$ nanoparticles. Nanomater-Basel. 2019;9(12):1697.
37. Panomsuwan G, Manuspiya H. Correlation between size and phase structure of crystalline $BaTiO_3$ particles synthesized by sol-gel method. Mater Res Express. 2019;6(6):065062.
38. Yan YJ, Xia H, Fu YQ, et al. Controlled hydrothermal synthesis of different sizes of $BaTiO_3$ nanoparticles for microwave absorption. Mater Res Express. 2020;6(12):1250i3.
39. Jin MH, Shin E, Jin S, et al. Solvothermal synthesis of ferroelectric $BaTiO_3$ nanoparticles and their application to dye-sensitized solar cells. J Korean Phys Soc. 2018;73(5):627–631.
40. Rostamzadeh T, Adireddy S, Wiley JB. Formation of scrolled silver vanadate nanopeapods by both capture and insertion strategies. Chem Mater. 2015;27(10):3694–3699.
41. Caruntu D, Rostamzadeh T, Costanzo T, et al. Solvothermal synthesis and controlled self-assembly of monodisperse titanium-based perovskite colloidal nanocrystals. Nanoscale. 2015;7(30): 12955–12969.
42. Bu WB, Chen ZX, Chen F, et al. Oleic acid/oleylamine cooperative-controlled crystallization mechanism for monodisperse tetragonal bipyramid $NaLa(MoO_4)(2)$ nanocrystals. J Phys Chem C. 2009; 113(28):12176–12185.
43. Sun SH, Murray CB, Weller D, et al. Monodisperse FePt nanoparticles and ferromagnetic FePt nanocrystal superlattices. Science. 2000;287(5460):1989–1992.